Effect of ZnO coating on physicochemical properties of $LiFePO_4$ cathode material for lithium ion batteries

Rakesh Saroha, Aditya Jain, A. K. Panwar*

Department of Applied Physics, Delhi Technological University, Delhi, 110042, India

*Corresponding author, E-mail: panwaramar@gmail.com; Tel: +91-9891778307

Received: 31 March 2016, Revised: 27 July 2016 and Accepted: 03 August 2016

DOI: 10.5185/amp.2016/118
www.vbripress.com/amp

Abstract

The effects of ZnO nanoparticle coating on the physicochemical and electrochemical properties of $LiFePO_4$ (LFP) have been investigated in this work. ZnO-modified $LiFePO_4$ cathode materials were synthesized via sol-gel and modified by ZnO nanoparticle using ball mill method. The amount of ZnO additive is chosen as a controlling factor to tune ZnO content over the surface of LFP particles. Structure and morphology of the LFP material with and without ZnO-coating layer were studied using X-ray diffraction (XRD), scanning electron microscopy (SEM) and Fourier transform infrared (FTIR) spectra. The XRD patterns reveal that the proper phase of LFP is formed with the ordered olivine-type orthorhombic structure of *Pnma* space group, and no impurity phase like $LiZnPO_4$ has been noticed. AC conductivity measurements have shown that the ZnO-modified LFP samples significantly assists in lowering the resistance of cathode active material and enhancing the conductivity. It is found that the 2.5 wt% ZnO-doped LFP exhibits the highest conductivity than the 5 wt% ZnO and 1 wt% ZnO doped LFP or the un-doped sample**.** Among the synthesized samples, LFPZ2.5 displays highest discharge capacity 160 (±5) $mAhg^{-1}$ (~94% of the theoretical capacity of $LiFePO_4$) at 0.1C rate. These results indicate that 2.5 wt% ZnO coated pristine LFP sample proves to be alternative material for automotive industry and it may be possible alternate of cathode materials in hybrid electric vehicles. Copyright © 2016 VBRI Press

Keywords: Olivine, sol-gel, ZnO-modified LFP, conductivity, electrochemical performances.

Introduction

Olivine-type $LiFePO_4$ proves to be one of the most promising cathode material for lithium ion batteries. It has undergone extensive research since it was first reported by padhi et al. in 1997 [**1**]. It satisfies most of the requirements of high theoretical capacity (170 $mAhg^{-1}$), low cost and environmentally benign due to its non-toxicity [**2-5**]. The $(PO_4)^{3-}$ tetrahedral structure unit present in olivine structure modify the redox potential of the $Fe^{2+/3+}$ couple and thus producing steady voltage plateau at around 3.4 V vs. Li^+/Li [**3, 4**]. However, low electronic conductivity (10^{-9} – 10^{-11} S cm^{-1}) and poor electrochemical performances of pristine $LiFePO_4$ has restricted its commercial use in automotive industry for EVs and HEVs. Various ways have been adopted till date to increase the conductivity and electrochemical properties of pristine $LiFePO_4$ cathode material which mainly includes carbon coating [**6**] and cation doping at the M1/M2 site [**7,8**]. Apart from this, conductivity can also be enhanced by coating/ surface modification of pristine $LiFePO_4$ material with electronically conductive materials such as $LaPO_4$ [**9**], CuO [**10**], NbC [**11**], LTO [**12**] and much more.

Carbon coating has been widely applied to tune morphology of cathode active material. Apart from conducting carbon coating, there are various reports on metal oxides coatings of $LiFePO_4$ material [**10, 13**]. Zinc oxide (ZnO) one of the metal oxides, when coated over the surface of lithium iron phosphate particles assists lithium ion diffusion and increases electrochemical performances of pristine $LiFePO_4$. Incorporation of Zn into $LiFePO_4$ lattice induces some kind of "pillar effect" which provides more space for lithium ion movement and consequently, the conductivity of $LiFePO_4$ is enhanced [**13**]. Cui et al. [**14**] studied the effect of ZnO/C co-coated on the electrochemical properties of $LiFePO_4$ cathode material and revealed that ZnO-$LiFePO_4$ sample shows highest current exchange density and maximum discharge capacities of 147.7 $mAhg^{-1}$ and 138.5 $mAhg^{-1}$ at 1C and 2C rates, respectively. Hu et al. [**13**] studied ZnO-doped $LiFePO_4$ synthesized by hydrothermal method and found that ZnO-doped sample exhibits a discharge capacity of 132.3 $mAhg^{-1}$

and 80 $mAhg^{-1}$ at 0.1C and 1C, respectively. TANG et al. [**15**] investigate aluminum doped zinc oxide coated $LiFePO_4$ material and observed discharge capacities of 165.8 $mAhg^{-1}$ and 158.1 $mAhg^{-1}$ at 0.1C and 1C, respectively in a charge/discharge voltage window of 4.0-2.0 V. However, there is no information available on the microstructure and electrochemical properties of the ZnO coating with different wt.% over the surface of pristine LFP, which prompted the authors to investigate the present composition.

The objective of this work is to investigate the effects of a surface coating of ZnO nanopowder on the surface of pristine $LiFePO_4$. The effect of a surface coating by ZnO over the surface of pristine $LiFePO_4$ has been systematically studied in terms of physicochemical and electrochemical properties. All the samples were synthesized using the sol-gel assisted ball-milling route with sucrose (10 wt %) as a carbon source. Physicochemical characteristics of the synthesized samples were examined by using XRD, SEM, and FTIR. Electrochemical characterization of as-prepared samples is carried out to investigate electrochemical properties.

Experimental

Materials

Pristine lithium iron phosphate ($LiFePO_4$) and ZnO-coated samples were synthesized by sol-gel route followed by ball-milling for ZnO coating. Stoichiometric amounts of $LiOH.H_2O$ (Sigma-Aldrich, U.S.A, ≥99%), $Fe(NO_3)_3.9H_2O$ (CDH, New Delhi, 98%) and $H_9N_2O_4P$ (Sigma-Aldrich, U.S.A, ≥99%) were used as precursors while sucrose GR (Mumbai, MERCK) was used as additive for carbon source and as a reducing agent. Citric acid (Sigma-Aldrich, U.S.A, ≥98%) was used as chelating agent.

Method

Separate solutions of all the precursors in deionized water were prepared and then added to the citric acid solution. The resulting solution of citric acid and precursors was heated at 70 ºC at 400 rpm with continuous stirring till a transparent gel was obtained. The gel thus obtained was decomposed at 350 ºC for 5 h in a tubular furnace under reducing atmosphere. The yielded powder after decomposition was reground together with ZnO and sucrose. Then it was ball milled for 2 h at 400 rpm in toluene media. The final product was obtained by calcination of the mixture at 750 ºC for 12 h in slightly reducing atmosphere of Ar/H_2. The pristine $LiFePO_4$ and coated with 1.0, 2.5, 5.0 wt % of ZnO nanoparticles were named as LFP, LFPZ1, LFPZ2.5and LFPZ5.

ZnO nanopowder was synthesized by a wet chemical method using Zinc acetate dihydrate ($(CH_3COO)_2$ $Zn.2H_2O$) as a precursor. Zinc acetate dehydrate was dissolved in deionized water with continuous stirring at 40 ^{0}C. After few hours of stirring a white powder was obtained which is subjected to calcination at 450 ^{0}C for 24 hours in order to get ZnO nanopowder.

Electrode preparation and electrochemical characterization

Synthesized samples were characterized using RIGAKU make X-ray diffractometer of CuK_α radiation (λ=1.54178 Å) for crystal structure and phase composition analysis. Rietveld refinement was done using X'pert high score plus software. The morphological study was carried out using HITACHI make scanning electron microscope of model S-3700 N. The Fourier transform infrared (FTIR) spectra were recorded with a PERKIN ELMER (C91158) make spectrometer in the wavenumber range of 1400–400 cm^{-1}. A two-point probe setup (AGILENT 4284A) was used to measure the electronic conductivity of the synthesized samples at a bias voltage of 1.0 V and in the frequency range of 20 Hz-1MHz. The electronic conductivity (σ) is calculated by using following equation

$$\sigma = \frac{1}{R}\left(\frac{L}{A}\right)$$

where, R is the resistance of the sample (**Ω**), L and A is thickness (cm) and cross-sectional area (cm^2) of the pellets respectively. For electrochemical studies, electrodes were prepared by preparing slurries of the active material, conductive carbon and binder (PVDF) with a weight ratio of 70:15:15 in N-methyl-2-pyrrolidinone (NM2P) as a solvent. The resulting slurry was then coated on Al foil using "doctor blade" technique. The coating was dried in a vacuum oven for overnight to evaporate the solvent. The electrodes were then punched and dried under vacuum at 60 ºC and finally brought inside the glove box Mbraun make (O_2 and H_2O level below 0.5 ppm). The coin cells (CR2032) were assembled for electrochemical testing of the synthesized samples. A microporous polypropylene sheet (Celgard 2400) was used as a separator and the electrolyte used was 1 M $LiPF_6$ in EC: DMC 1:1 v/v. High purity Li chips were used as both counter and reference electrode. The galvanostatic charge/discharge (GCD) performance test was performed at 0.1C-rate. All the electrochemical tests were performed using EZstat-pro Nuvant systems Inc. (U.S.A) cell test system at 298 K (RT).

Results and discussion

Structural and Morphological Analysis

The XRD patterns of the as-synthesized samples with different ZnO amount are shown in **Fig. 1**. From XRD patterns, it is found that all the diffraction peaks can be well indexed to orthorhombic phase with *Pnma* space group of olivine-$LiFePO_4$. The sharp peaks for all the synthesized samples indicate that the

samples are well crystalline in nature. No impurity phase like $LiZnPO_4$ has been detected in the synthesized samples. The unit cell parameters and unit cell volume of all the synthesized samples are listed in **Table 1**.

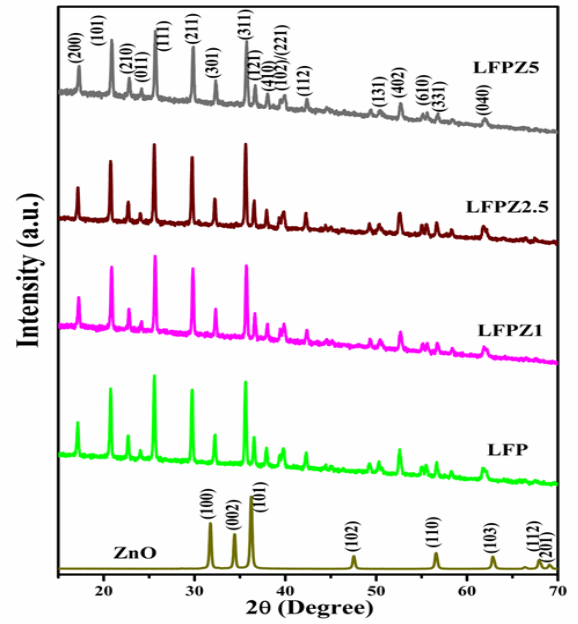

Fig. 1. XRD patterns of the LFP-ZnO synthesized samples.

From **Table 1**, it can be seen that for ZnO-coated samples, unit cell parameters, and unit cell volume increases as compared to the pristine LFP. The increase in cell size from 289.426 to 290.977 $(Å)^3$ is mainly due to a slight increase in lattice parameter *b* and *c* whereas *a* decrease slightly. It has been reported previously that introduction of Zn into $LiFePO_4$ lattice introduce some kind of "pillar effect" which provides more space for lithium ion movement and consequently, the conductivity of $LiFePO_4$ is enhanced and so its lithium ion diffusion coefficient [**13, 16**]. The increase in unit cell size, thus offer more space for lithium ion movement and consequently improved electrochemical properties.

Table 1. Results of the lattice parameters for LFP-ZnO synthesized samples. All distance and lattice parameters units are in Å (10-10 m).

Sample	a (Å)	b (Å)	c (Å)	V $(Å)^3$
LFP	10.307	5.995	4.684	289.426
LFPZ1	10.315	6.001	4.690	290.312
LFPZ2.5	10.312	5.999	4.689	290.069
LFPZ5	10.297	6.015	4.698	290.977

Fig. 2(a-e) shows the effect of a surface coating by ZnO on the morphology of the synthesized samples. It can be seen from **Fig. 2(a)** that the grains in the pristine $LiFePO_4$ sample are highly agglomerated possess nearly spherical morphology and are micrometer in size (~ 1 μm). **Fig. 2(b-d)** shows that ZnO coated samples are found to have grains with a smaller size (~500-700 nm) and are also uniformly distributed. Therefore, the concentration of alien dopant plays a crucial role in controlling the morphology of synthesized samples. **Fig. 2(e)** shows the SEM micrograph of ZnO nanoparticles. The size of ZnO nanoparticles lies between 50-100 nm and are homogeneously distributed.

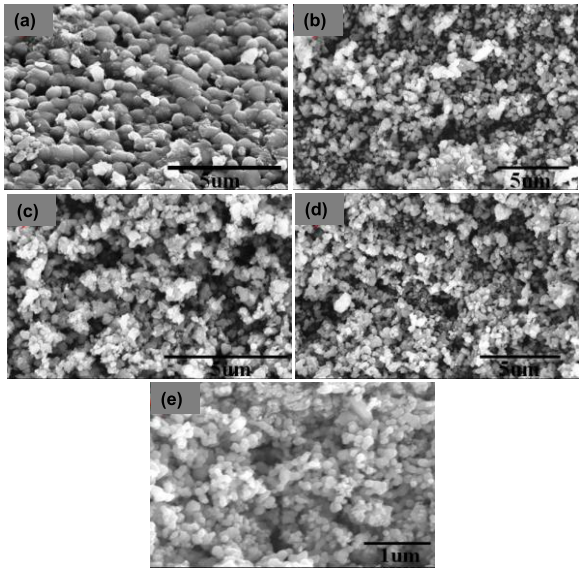

Fig. 2. SEM micrographs of LFP-ZnO synthesized samples (a) LFP; (b) LFPZ1; (c) LFPZ2.5; (d) LFPZ5; (e) ZnO.

FTIR study- Cation environment

The motion of cations with respect to the oxygen atom is generally assigned by vibrational modes which are much sensitive to the point group symmetry of the cations in the oxygen host matrix [**17**]. Therefore, the cations local environment in a crystal lattice of close-packed oxygen atoms can be analyzed using FTIR spectroscopy. It has been reported previously that alkali metal cations in their octahedral interstices (LiO_6) present in inorganic oxides have their resonant frequencies present in the frequency range of 200-400 cm^{-1}. The effect of ZnO coating on the vibrational spectrum of the LFP is investigated by FTIR and results are shown in **Fig. 3**.

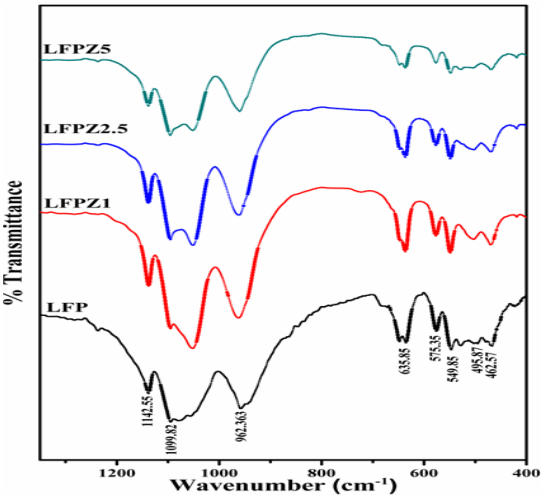

Fig. 3. FTIR spectrum of LFP-ZnO samples in a range of 400-1500 cm^{-1}.

The peaks of FTIR spectrum located from 463-1139 cm^{-1} may be attributed to the bending and stretching vibration of the tetrahedral (PO_4^{3-}) ion. The tetrahedral unit, (PO_4^{3-}) ion has its fundamental vibrational frequencies at 1082, 515, 980 and 363cm^{-1} [**17**]. Small peak around 420cm^{-1} corresponds to the stretching E2 (LO) mode of ZnO wurtzite structure as reported by Husain et al. [**18**]. Therefore, FTIR spectra reveal the presence of ZnO over LFP particles surface.

Electronic conductivity measurements

The conductivity (AC) of pristine LFP is found to be of the order 10^{-9} S cm^{-1}, which is in good agreement with the previous reports [**9**]. **Fig. 4** reveals the AC electrical resistance measurement for all the synthesized samples in the frequency range of 20 Hz-1MHz. The intercept at Z'-axis gives the AC resistance of the material.

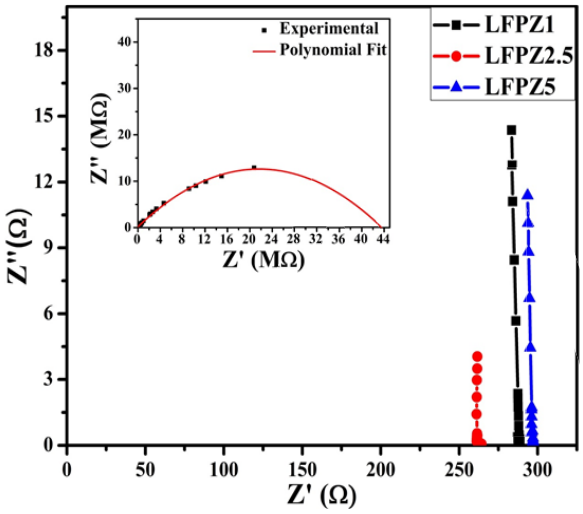

Fig. 4. AC Conductivity measurements of ZnO-coated synthesized samples in a frequency range of 20 Hz-1MHz.

From **Table 2**, it is evident that AC resistance measurement shows the pure conducting nature of ZnO-coated LFP samples. An increase of 10^5 in electronic conductivity has been obtained by coated samples. The tremendous increase in ZnO-coated LFP samples could be attributed to the presence of dangling bonds in ZnO, as zinc oxide quickly adsorb O^{2-} and O^- ions on its surface which consequently alter the surface energy and hence, the surface potential of active particle i.e. LFP [**19**].

Table 2. Parameters for the conductivity of LFP-ZnO synthesized samples.

Sample	$R_{A.C}$ (Ω)	$\sigma_{A.C}$ (S cm^{-1})
LFP	$43x10^6$	$4.95x10^{-9}$
LFPZ1	288	$7.98x10^{-4}$
LFPZ2.5	261	$8.22x10^{-4}$
LFPZ5	296	$7.17x10^{-4}$

Electrochemical performance of ZnO-coated LFP samples

Table 3 shows the initial galvanostatic charge/discharge curves of cells at 0.1C (1C = 170$mAhg^{-1}$) has been performed for the bare LFP and of all ZnO-LFP samples in the potential range of 2.0-4.4 V vs. Li^+/Li at room temperature. It is found that the discharge capacity of pristine $LiFePO_4$ is greatly enhanced by ZnO coating. Among all the synthesized samples LFPZ2.5 shows highest specific discharge capacity 160 (±5) $mAhg^{-1}$ (~94 % of theoretical capacity 170 $mAhg^{-1}$) because of its highest electronic conductivity. The discharge capacities of all samples for 0, 1.0, 2.5 and 5.0 wt % of ZnO amount are observed as 85 (±5), 128 (±5), 160 (±5) and 120 (±5) $mAhg^{-1}$, respectively. These results are fairly improved than previous studies [**13, 14, 20**]. The potential difference between charge and discharge plateaus for all the samples are shown in Table 3. It can be observed that the potential difference (ΔV) improved effectively with ZnO-coating. In other words, polarization potential reduces for ZnO-coated samples, indicating that reaction kinetics in $LiFePO_4$ have enhanced.

Hence, ZnO-coating over LFP surface effectively enhance the conductivity of pristine LFP and shows better electrochemical results as compared to pristine LFP.

Table 3. Galvanostatic Charge/Discharge parameters and Discharge capacity values of 1st charge/discharge cycle at 0.1C for LFP and ZnO-coated LFP samples.

Samples	Charge plateau Voltage (V)	Discharge plateau Voltage (V)	ΔV (V)	Discharge Capacity (mAh/g) (±5)
LFP	3.495	3.394	0.101	85
LFPZ1	3.469	3.395	0.074	128
LFPZ2.5	3.467	3.397	0.070	160
LFPZ5	3.496	3.379	0.117	120

Conclusion

The pristine $LiFePO_4$ and ZnO-coated $LiFePO_4$ samples were successfully synthesized using sol-gel assisted ball-milling method. XRD patterns reveal that all the synthesized samples are well crystalline and have orthorhombic lattice structure with *Pnma* space group. SEM images disclose the formation of nearly spherical shaped nano-sized particles. FTIR studies show the presence of vibrational modes corresponding to $(PO_4)^{3-}$ tetrahedral and stretching E2 (LO) mode of ZnO wurtzite structure. LFPZ2.5 shows the lowest resistance and, therefore, highest electrical conductivity which proves that it will possess best electrochemical kinetic properties among all the prepared samples. Galvanostatic charge/discharge curves confirm that LFPZ2.5 gives the highest discharge capacity at 0.1C rate.

Acknowledgements

Authors are thankful to SERB and FIST, Department of Science and Technology (DST), New Delhi for financial support to carry out this work under the project grants Nos.: SR/FTP/PS-039/2011 and SR/FST/PSI-164/2011(C), respectively.

References

1. A.K. Padhi, K.S. Nanjundaswamy, J.B. Goodenough; *J. Electrochem. Soc.* **1997**, *144*, 1188-1194.
2. Yi-Ju Lv, Jing Su, Yun-Fei Long, Xiao-Ru Cui, Xiao-Yan Lv, Yan-Xuan Wen; *Powder Technol.* **2014**, *253*, 467-473.
3. Guohui Qin, Qianqian Ma, Chengyang Wang; *Electrochim. Acta* **2014**, *115*, 407-415.
4. Xiaoting Lin, Kaiqiang Wu, Lianyi Shao, Miao Shui, Dongjie Wang, Nengbing Long, Yuanlong Ren, Jie Shu; *J. Electroanal. Chem.* **2014**, *726*, 71-76.
5. B. Scrosati, Low voltage lithium-ion cells (chapter 10), Advances in Lithium-Ion Batteries, Walter A. Van Schalkwijk and Bruno Scrosati, ebook.
6. Jin Chong, Shidi Xun, Xiangyun Song, Paul Ridgway, Gao Liu, Vincent S. Battaglia; *J. Power Sources* **2012,** *200*, 67-76.
7. Xujiao Yang, Zhendong Hu, Jun Liang; *Ceram. Int.* **2015**, *41*, 2863-2868.
8. G.X. Wang, S. Bewlay, J. Yao, J.H. Ahn, S.X. Dou, H.K. Liu; *Electrochem. Solid-State Lett.* **2004**, *7 (12)*, A503-A506.
9. Zhipeng Ma, Youshun Peng, Guiling Wang, Yuqian Fan, Jianjun Song, Tingting Liu, Xiujuan Qin; *Electrochim. Acta* **2015**, *156*, 77-85.
10. Yan Cui, Xiaoli Zhao, Ruisong Guo; *J. Alloys Compd*. **2010**, *490*, 236-240.
11. Jing Hu, Zaimin Tian; *Ceram. Int.* **2015**, *41*, 3927-3931.
12. Chun-Chen Yang, Jer Huan Jang, Jia-Rong Jiang; *Appl. Energy* **2016**, *162*, 1419-1427.
13. Yemin Hu, Jun Yao, Zhe Zhao, Mingyuan Zhu, Ying Li, Hongming Jin, Huijun Zhao, Jiazhao Wang; *Mater. Chem. Phys.* **2013**, *141*, 835-841.
14. Yan Cui, Xiaoli Zhao, Ruisong Guo; *Mater. Res. Bull.* **2010**, *45*, 844-849.
15. Hao TANG, Long TAN, Jun Xu; *Trans. Nonferrous Met. Soc. China* **2013**, *23*, 451-455.
16. Atef Y. Shenouda, Hua K. Liu; *J. Alloys Compd.* **2009**, *477*, 498-503.
17. N. Jayaprakash, N. Kalaiselvi; *Electrochem. Commun.* **2007**, *9*, 620-628.
18. Sajid Husain, F. Rahman, Nasir Ali, P. A. Alvi; *Journal of Optoelectronics Engineering* **2013**, Vol. 1, No. 1, 28-32.
19. Rakesh Saroha, A. K. Panwar; *Adv. Sci. Lett.* **2015**, *21*, 2750-2754.
20. Jungbae Lee, Purushottam Kumar, Jinhyung Lee, Brij M. Moudgil, Rajiv K. Singh; *J. Alloys Compd.* **2013**, *550*, 536-544.

